Size-dependent ferroic phase transformations in GeSe nanoribbons

Yang Yang[1], Hongxiang Zong[1,*], Xiangdong Ding[1,*], Jun Sun[1]

[1.] *State Key Laboratory for Mechanical Behavior of Materials, Xi'an Jiaotong University, Xi'an 710049, China*

[*] Authors to whom correspondence should be addressed:

zonghust@mail.xjtu.edu.cn (H.Z.)
dingxd@mail.xjtu.edu.cn (X.D.)

Abstract: Ferroic phase transformation in monolayer nanosheets or nanoribbons endows 2D nanoelectronic devices with novel functionalities. However, less is known how the phase transformation behaves with the system size. Combined with molecular dynamic simulations and machine learning model, we systematically investigate the temperature induced ferroic phase transformation in monolayer GeSe nanoribbons, which exhibits remarkable size effect. Specifically, the transformation hysteresis is found continuously decreased with ribbon width at the investigated scales. In contrast, the transformation temperature of monolayer GeSe nanoribbon shows a non-monotonic size-dependency, i.e., it is first increased and then decreased as we narrow the GeSe nanoribbons. We attribute this to a competition between the enhanced ripple deformation, which will promote phase transformation upon cooling, and the stronger edge effect that can suppress phase transformation. What's more, the two factors are well captured by the Landau model, which will deepen our understanding on phase transformation behaviors in 2D ferroic materials.

The past two decades have witnessed the fantastic discoveries of multifunctional two-dimensional (2D) materials [1-5]. Among them, 2D ferroic materials such as 1T' WTe2 [6], black phosphorene [7], group IV monochalcogenides [8-10] etc. exhibit fascinating properties due to the ferroic phase transformation and domain switching. Group IV monochalcogenides [8-11]e.g. GeSe monolayers, as a typical 2D multiferroic material, show strong coupled ferroelastic-ferroelectric orders. Below the phase transformation temperature (typically < 300 K [11]), it shows spontaneous strain or polarization and domain patterns [9], which have been observed experimentally [12-14], serving as an ideal case to understand the phase transformation behaviors in 2D materials.

A class of native structures named ripples [15], which originate from the low-energy flexural out-of-plane bending mode, widely exist in 2D materials, including 2D ferroic materials [10,15-19]. Different from the static ripples induced by deformed substrate in 3D bulk membranes, ripples in 2D materials are intrinsic and with ultrafast dynamics [19]. Static ripples in 3D bulk ferroic membranes induced out-of-plane strain field, resulting in a strong room-temperature ferroelectricity [20] and enhanced piezoelectricity [21]. However, the understanding of the dynamic rippling effects in 2D ferroics is still far from complete. Our previous work focused on the dynamic rippling effects on the phase transformation and domain switching in monolayer GeSe. We have indicated that the ripple deformation can help stabilize low-temperature ferroic phase and increase the phase transformation temperatures [10]. Nevertheless, it is still unknown what the rippling effects look like in 2D ferroics with limited sizes (i.e. with free edges).

Free edges or surfaces work for the size effects of ferroic materials. For example, the structural phase transformation in 3D shape memory materials (typical ferroelastic materials) shows strong dependence of system size at small scale. Previous studies also demonstrate that shape memory alloys (SMAs) can exhibit different properties at small scale than their bulk counterparts, as manifested by suppressed phase transformation temperatures [22], and slim thermal or superelastic hysteresis in nano-scale SMAs [23,24]. The decreasing phase transformation hysteresis comes from the weak spontaneous strain and spatial heterogeneity in smaller system, which results in a quasi-continuous phase transformation process [24]. However, less is known whether it is the same true for 2D shape memory or ferroic materials.

2D ferroic materials possess several unique aspects that are different from that in 3D bulk materials [25]. Often, 2D ferroic materials have a thickness of several atomic layers, which gives rise

to strong surface effects along the out-of-plane direction. Cutting the 2D nano-sheet of ferroic materials into nanoribbons leads to additional changes from edge effect. Furthermore, 2D materials are featured by unique flexible bending mode, resulting in inborn ripple deformation [10,15-19]. The motivation of this work is to understand how these effects change with the system size and their role in the phase transformations of 2D ferroic materials.

In the present work, molecular dynamics (MD) simulation is carried out to study structural phase transformations in monolayer GeSe nanoribbons, aimed at achieving an atomic-level understanding of the size effect on 2D shape memory materials. The atomic interaction in monolayer GeSe is described by a machine learning potential that are directly learned from high-accuracy first-principle calculations [10]. Our previous work has shown that the machine learning potential can exactly reproduce the ferroic phase transformation and domain switching processes in GeSe monolayer. Typical GeSe nanoribbons are created with a system size of 15.9 nm in length and 4.0~17.0 nm in width, containing up to 6400 atoms. The periodic boundary condition is only applied along the nanoribbons while the other two directions are bounded by two free surfaces. All the samples are first relaxed at 200 K by using a Nose-Hoover thermostat [26,27] and Parrinello–Rahman barostat [28] within the isothermal-isobaric ensemble. After this procedure, we performed MD simulations of cooling and heating on the annealed samples utilizing the LAMMPS code [29]. The cooling and heating processes involve cyclic increase or decrease in temperature with rates of 0.5 K/ps. The complete details of the machine learning model and the code for LAMMPS implementation has been uploaded to https://github.com/yangymse/GeSe-MLPotential.git.

Fig. 1(a) shows the crystal structure of low-temperature ferroic phase, whose formation can be characterized by the changes in the lattice parameter a and b, as well as the relative in-plane displacement vector between Ge-Se pairs (Δx, Δy). The local lattice-invariant shear (i.e., a-b) differs ferroelastic domains or variants with different symmetry-equivalent directions of structural distortion while the displacement vector of (Δx, Δy) quantify local spontaneous polarization, as shown in Fig. 1(b). GeSe monolayer has four different variants associated with the symmetry change upon phase transformation at low temperature. In Fig. 1(c), we show a single ferroelastic domain with local spontaneous strain along y direction after the phase transformation, and the arrows represent local spontaneous polarization. Note that the spatial distribution of local spontaneous strain and spontaneous polarization is correlated, indicating a strong coupling

between them [7,9]. Therefore, either one in our case can be used as the order parameter of phase transformation in monolayer GeSe. At high temperature, both order parameters in monolayer GeSe lost their long-range order (Fig. 1(d)), which suggests the occurrence of a structural phase transformation upon heating. Even so, we still can see very weak short-range ferroic order in high-temperature phase due to the presence of local ripple deformation [10].

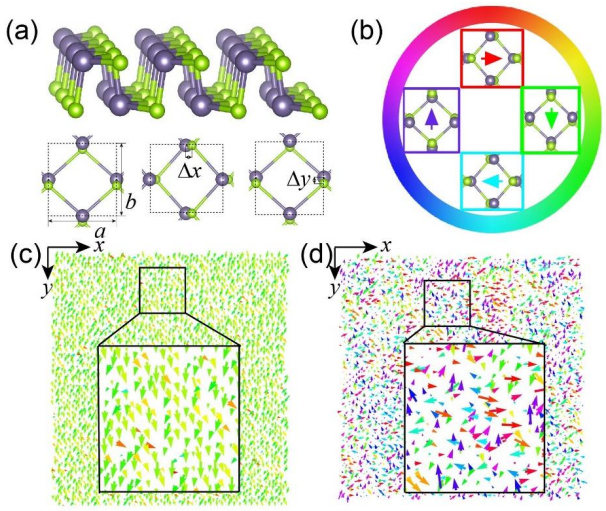

FIG. 1. Structural changes upon the phase transformation in monolayer GeSe. (a) Atomistic configurations and selected order parameter in ferroic monolayer GeSe. (b) The four symmetry-equivalent directions of structural distortion in the low-temperature phase are indicated by the displacement vector of (Δx, Δy). (c) Single domain structure of low temperature phase. (d) High temperature phase with weak short-range ferroic order. The arrows represent relative in-plane displacement of (Δx, Δy) between Ge-Se pairs.

Our work started by studying the stable monolayer GeSe nanoribbons. Here, both the armchair and zigzag edged GeSe nanoribbons are considered. As shown in Fig. S1, we designed two types of pristine monolayer GeSe nanoribbons with either armchair or zigzag edges. When undergoing phase transformation upon heating or cooling, the edges in both cases transform into zigzag. It indicates that the zigzag edge is more stable in monolayer GeSe nanoribbons. This is further confirmed by the edge energy calculation. By means of first principle calculations, we show that the zigzag edged nanoribbon has an edge formation energy of 903 meV/nm, which is lower

than that of armchair edged nanoribbons (1182 meV/nm). Therefore, our study hereafter will focus on the zigzag edged GeSe nanoribbons.

Fig. 2 shows the size dependence of phase transformation behaviors in GeSe nanoribbons. In detail, zigzag edged GeSe nanoribbons with ribbon width varying from 4 nm to 16 nm as well as a freestanding GeSe nanosheet are involved in our MD simulations. Fig. 2(a) shows the temperature dependent mean lattice parameter *a* and *b* upon heating and cooling. The difference between *a* and *b* reflects the symmetry change associated with the phase transformation in GeSe. Under cooling, both *a* and *b* decrease smoothly with temperature. Then a discontinuous change occurs due to the occurrence of a first-order phase transformation. The corresponding phase transformation temperature is defined as the martensitic starting temperature (M_s). Similarly, when we heat the samples, the *a* and *b* will vary continuously first, then coincided at the reverse phase transformation temperature, which is known as the austenite finishing temperature (A_f). Usually, the austenite finishing temperature is higher than the martensitic starting temperature, and their difference can be used to evaluate the phase transformation hysteresis (A_f-M_s).

Fig. 2(b) shows the forward and reverse transformation temperatures (M_s and A_f, respectively) of the GeSe nanoribbons. Compared with the monolayer GeSe nanosheet (~320 K, as shown in Fig. 2(a)), A_f in GeSe nanoribbons is slightly decreased first. However, the change in A_f become sharp as the nanoribbons is narrow than 8 nm. More differently, the size dependence of M_s shows a "Λ" shape. With reducing width of GeSe nanoribbons, the M_s first rises above 8 nm, then decreases sharply. It is important to note that such non-monotonic size dependency of M_s has never been observed in bulk shape memory materials [24]. Moreover, the transformation hysteresis ΔT (here we define $\Delta T = A_f - M_s$) becomes smaller with reducing size, as shown in Fig. 2(c), be consistent with previous observation in shape memory alloys [24].

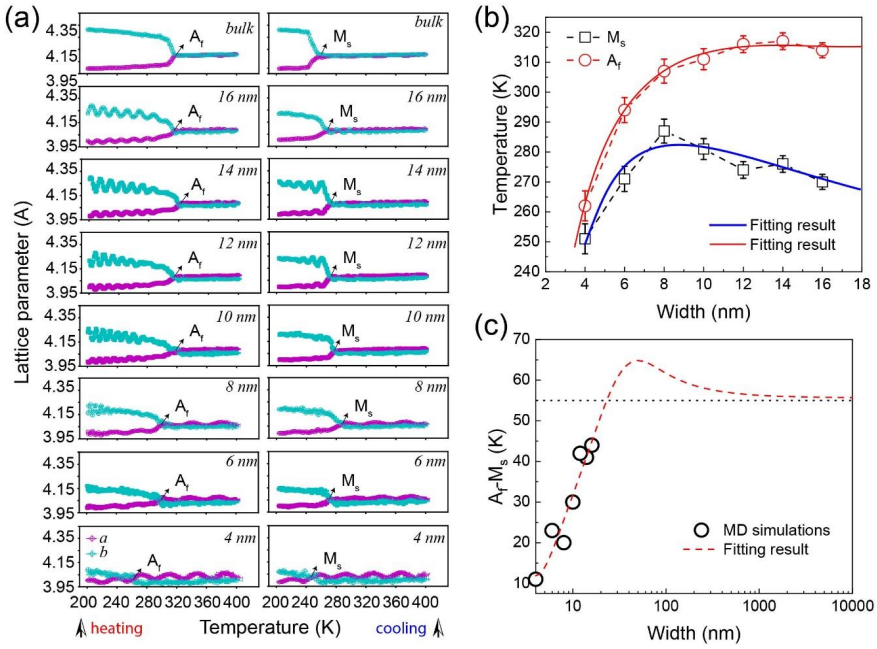

FIG. 2. Size dependency of ferroic phase transformations in monolayer GeSe nanoribbons. (a) Mean lattice parameters as a function of temperature upon heating and cooling. (b) The nanoribbon width-dependent transformation temperatures (M_s and A_f). Landau-type analysis model showing the relationship between M_s (blue solid line) and A_f (red solid line) and ribbon width. They agree well with the MD simulation results. (c) The corresponding transformation hysteresis as a function of the ribbon width during the forward and reverse phase transformations. Once the system is approaching the bulk limit, the hysteresis saturated at 55 K (red dashed line).

To reveal the microscopic nature of size effect, we investigate the corresponding microstructure evolution upon heating and cooling in a GeSe nanoribbon. By examining multiple snapshots stored during the MD simulations, we find that the phase transformation process in GeSe nanoribbons is strongly related to the regions near the ribbon edges. As shown in the upper panel of Fig. 3, the high-temperature phase prefers to nucleate from the near-edge regions upon heating, and then grow into the whole sample (Fig. 3(a)-(d)). In contrast, when we decrease the temperature

from high-temperature phase region, the low-temperature phase prefers to nucleate from the ribbon inner, instead of the edges. A further cooling leads to the entirely low-temperature phase with multi-domain structure, see the lower panel of Fig. 3(e)-(h). Even so, the spontaneous strain or polarization in the near-edge regions is much weaker than the center place. Our findings thus suggest that the edge plays an important role in the phase transformation process in 2D GeSe nanoribbons.

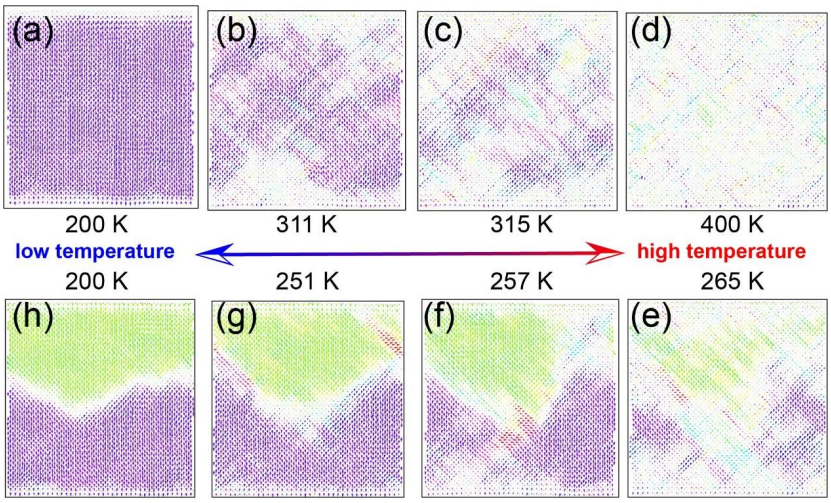

FIG. 3. Typical atomic configurations of a GeSe nanoribbon with zigzag edges upon heating and cooling. (a) Original single domain structure. (b)-(d) Nucleation and growth of high-temperature phase upon heating. (e)-(h) Nucleation and growth of low-temperature phase upon cooling.

Coincidentally, previous results found that surface regions dominate the phase transformation in nano-scale shape memory materials [22]. Accordingly, we calculated the formation energy of ribbon edges in martensite (γ^{M}) and austenite (γ^{A}). In our MD simulations, the edge formation energy is calculated by $\gamma_{edge} = (E_{free} - E_{peri})/N$, where E_{free} represents the total potential energy of a GeSe nanoribbon system while E_{peri} is the corresponding potential energy of GeSe bulk, and N is the atom number of the system. As expected, the edge formation energy in low-temperature phase (γ^{M}) is higher than that in high-temperature phase (γ^{A}). This indicates that the spontaneous strain/polarization on the edges should be suppressed. Additional energetic price should be paid

for the formation of low-temperature phase in the near-edge regions. In other words, the low-temperature phase prefers to nucleate at the ribbon inner upon cooling while the high-temperature phase will start from the edges during the heating process. However, the nucleation of high-temperature phase in the near-edge region will be energetically preferred compared to its bulk counterpart. Furthermore, we find that the edge formation energy difference ($\Delta\gamma$) between low-temperature and high-temperature phase is enlarged with decreasing the sample size, as shown in Fig. 4(a). It should justify the suppressed phase transformation in narrower GeSe nanoribbons.

The out-of-plane deformation or ripple deformation in 2D materials makes additional contribution to the change of phase transformations in GeSe nanoribbons. Ripples are an intrinsic crystal defects in 2D materials, and involves locally with time and space [19]. This dynamic local deformation can induce local strain that facilitates local phase transformation in monolayer GeSe [10]. To uncover the role of ripple deformation in GeSe nanoribbons, we evaluate the intensity of ripple deformation as a function of system size. Here, both the Gaussian curvature κ and out-of-plane fluctuations [30] $\langle h^2 \rangle / S_0$ (S_0 refers to the initial area of the sample) due to ripple deformation are estimated, as shown in Fig. S2 and Fig. S3. Both increase exponentially with the reduction of ribbon width, indicating that the out-of-plane ripple deformation roughly follows an exponential relationship with the system size (Fig. 4(b) and S3(c)). As presented in our previous work [10], ripples introduce local random strain field, which can give rise to dynamic low-temperature phase nano-regions even at high temperatures. The presence of ripples can extend the lifetime of local low-temperature phase about 100 times longer. With such enhanced ripple deformation at smaller sample, the low-temperature phase can be more stable at a higher temperature. It explains the increased M_s in narrower GeSe nanoribbons below 8 nm in Fig. 2(b). Besides the size-dependency, previous studies have shown that ripple deformation follows a linear relationship with temperature [10,30].

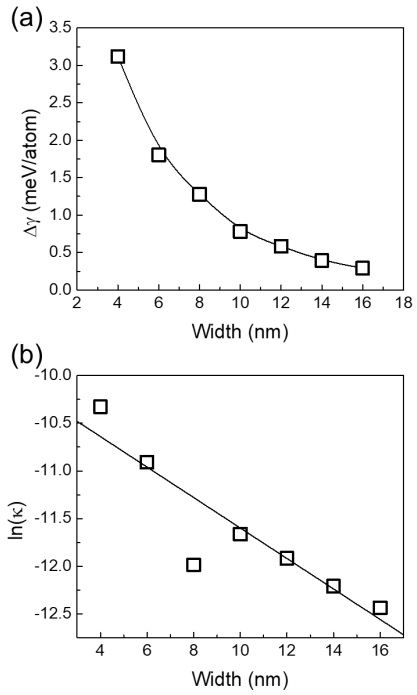

FIG. 4. Size effect on (a) Edge formation energy difference and (b) Mean Gaussian curvature in GeSe nanoribbons.

Thus, by taking account of the two factors, we propose a Landau-type model to study generally the structural phase transformations in monolayer GeSe nanoribbons. Previous studies have indicated that the surface/edge effect can be described by a phenomenological parameter, i.e., extrapolation length δ (>0) to characterize the near-edge region which favors the high-temperature phase [23,24]. The contribution of ripple deformation is related to additional strain energy due to phase transformation. Based on these, the Landau free energy of structural phase transformation in 2D materials can be expressed as,

$$F = \frac{1}{2}A\eta^2 + \frac{1}{4}B\eta^4 + \frac{1}{6}C\eta^6 + \frac{1}{2}s(\nabla\eta)^2 + r(W,T)\eta \quad (1)$$

where η is the order parameter; A, B and C are parameters related to the materials; A can be expressed as $A_0(T\text{-}T_c)$; $\frac{1}{2}s(\nabla\eta)^2$ is related to the surface inhibition to the martensitic phase transformation. $r(W,T)$ is the strain field induced by ripple deformation, where W and T refer ribbon width and temperature, respectively. Our previous work has shown that the strength of local strain field $r(W,T)$ is a linear function of order parameter η and temperature T [10]. By using similar strategy shown in Ref. [22] (see supplementary materials), the relationship between the martensitic phase transformation start temperature M_s and the ribbon width W can be obtained as

$$M_s = T_c^M - \frac{2s}{\delta W A_0} + \frac{1}{A_0} e^{mW} \quad (2)$$

The austenite phase transformation finish temperature can be obtained as

$$A_f = T_c^A - \frac{2s}{\delta W A_0'} + \frac{1}{A_0'} e^{m'W} \quad (3)$$

As shown in Fig. 2(b), we fit the simulation results with the Eq. (2) and (3), and the low fitting error indicates that our model can well capture the size dependence of phase transformation in GeSe nanoribbons.

The hysteresis (A_f-M_s) can be easily derived by substituting Equation R1 and R2, leading to Eq. (4):

$$A_f - M_s = (T_c^A - T_c^M) + p \cdot W^{-1} + q \cdot e^{l \cdot W} \quad (4)$$

where p, q and l are the reduced coefficients.

As the Eq. (4) suggested, once the system is approaching the bulk limit, the hysteresis saturated at 55 K (Fig. 2(c)), agrees well with our MD simulations.

Based on the analytical model, the structural phase transformations of real SMAs at nanoscale and their critical sizes could be estimated since the parameters in the present model can be obtained from experiments. The extrapolation length δ can be measured directly from high-resolution TEM images while other parameters can be obtained from the transformation properties of bulk materials. However, the Landau model cannot capture the effects of layer-thickness on the phase transformation. Thickness effects include: first, the adjacent layers should have opposite ferroelectric order parameters but the same ferroelastic order parameters. In this scenario, only

samples with odd layers show ferroelectricity [12,14]. Second, the ripple deformation is also thickness dependent [31]. Unfortunately, the current machine learning model cannot easily capture the interaction between GeSe layers, which could be studied in the future.

In summary, we have investigated the temperature induced ferroic phase transformation in 2D GeSe nanoribbons, which show strong size-dependency. Different from that in 3D shape memory materials, the phase transformation temperature shows non-monotonic size dependency in 2D GeSe nanoribbons. Atomic level investigations point out that the anomalous size effect results from a competition between the cost of additional edge formation energy and the promotion of ripple deformation induced local strain. The latter is unique for 2D shape memory materials. Due to the structural transformation in wide 2D ferroic materials, our findings potentially have board applications in 2D functional nano-systems such as shape memory effect, ferroelectric and magnetocaloric systems.

Supplementary Material

More details including the reconstruction of armchair free edge, size dependent curvature and out-of-plane fluctuations and the derivation of the Landau-type model can be found in the supplementary materials.

Acknowlegements

This work was supported by the National Natural Science Foundation of China (12104355, 51320105014, 51871177 and 51931004), the China Postdoctoral Science Foundation (2020M673385) and the 111 project 2.0 (BP2018008).

References

[1] Kostya S. Novoselov, Andre K. Geim, Sergei V. Morozov, D. Jiang, Y. Zhang, Sergey V. Dubonos, Irina V. Grigorieva, and Alexandr A. Firsov, science **306** (5696), 666 (2004).

[2] K. S. Novoselov, A. Mishchenko, A. Carvalho, and A. H. Castro Neto, Science **353** (6298), aac9439 (2016).

[3] Wonbong Choi, Nitin Choudhary, Gang Hee Han, Juhong Park, Deji Akinwande, and Young Hee Lee, Mater. Today **20** (3), 116 (2017).

[4] Yuan Cao, Valla Fatemi, Ahmet Demir, Shiang Fang, Spencer L. Tomarken, Jason Y. Luo, Javier D. Sanchez-Yamagishi, Kenji Watanabe, Takashi Taniguchi, and Efthimios Kaxiras, Nature **556** (7699), 80 (2018).

[5] Yuan Cao, Valla Fatemi, Shiang Fang, Kenji Watanabe, Takashi Taniguchi, Efthimios Kaxiras, and Pablo Jarillo-Herrero, Nature **556** (7699), 43 (2018).

[6] Wenbin Li and Ju Li, Nat. Commun. **7**, 10843 (2016).

[7] Menghao Wu and Xiao Cheng Zeng, Nano Lett. **16** (5), 3236 (2016).

[8] Ruixiang Fei, Wei Kang, and Li Yang, Phys. Rev. Lett. **117** (9), 097601 (2016).

[9] Hua Wang and Xiaofeng Qian, 2D Mater. **4** (1), 015042 (2017).

[10] Yang Yang, Hongxiang Zong, Jun Sun, and Xiangdong Ding, Adv. Mater. **33** (49), 2103469 (2021).

[11] Mehrshad Mehboudi, Benjamin M. Fregoso, Yurong Yang, Wenjuan Zhu, Arend van der Zande, Jaime Ferrer, L. Bellaiche, Pradeep Kumar, and Salvador Barraza-Lopez, Phys. Rev. Lett. **117** (24), 246802 (2016).

[12] Yang Bao, Peng Song, Yanpeng Liu, Zhihui Chen, Menglong Zhu, Ibrahim Abdelwahab, Jie Su, Wei Fu, Xiao Chi, and Wei Yu, Nano Lett. **19** (8), 5109 (2019).

[13] Naoki Higashitarumizu, Hayami Kawamoto, Chien-Ju Lee, Bo-Han Lin, Fu-Hsien Chu, Itsuki Yonemori, Tomonori Nishimura, Katsunori Wakabayashi, Wen-Hao Chang, and Kosuke Nagashio, Nat. Commun. **11** (1), 1 (2020).

[14] Kai Chang, Junwei Liu, Haicheng Lin, Na Wang, Kun Zhao, Anmin Zhang, Feng Jin, Yong Zhong, Xiaopeng Hu, and Wenhui Duan, Science **353** (6296), 274 (2016).

[15] A. Fasolino, J. H. Los, and M. I. Katsnelson, Nat. Mater. **6**, 858 (2007).

[16] Yi Wang, Rong Yang, Zhiwen Shi, Lianchang Zhang, Dongxia Shi, Enge Wang, and Guangyu Zhang, ACS nano **5** (5), 3645 (2011).

[17] L. Tapaszto, T. Dumitrica, S. J. Kim, P. Nemes-Incze, C. Hwang, and L. P. Biro, Nat. Phys. **8** (10), 739 (2012).

[18] Akihiro Kushima, Xiaofeng Qian, Peng Zhao, Sulin Zhang, and Ju Li, Nano Lett. **15** (2), 1302 (2015).

[19] Jianbo Hu, G. M. Vanacore, Andrea Cepellotti, Nicola Marzari, and Ahmed H. Zewail, Proc. Natl. Acad. Sci. U.S.A. **113** (43), 201613818 (2016).

[20] Tianyu Li, Shiqing Deng, Hui Liu, Shengdong Sun, Hao Li, Shuxian Hu, Shi Liu, Xianran Xing, and Jun Chen, Adv. Mater. **33** (21), 2008316 (2021).

[21] Guohua Dong, Suzhi Li, Tao Li, Haijun Wu, Tianxiang Nan, Xiaohua Wang, Haixia Liu, Yuxin Cheng, Yuqing Zhou, Wanbo Qu, Yifan Zhao, Bin Peng, Zhiguang Wang, Zhongqiang Hu, Zhenlin Luo, Wei Ren, Stephen J. Pennycook, Ju Li, Jun Sun, Zuo-Guang Ye, Zhuangde Jiang, Ziyao Zhou, Xiangdong Ding, Tai Min, and Ming Liu, Adv. Mater. **32** (50), 2004477 (2020).

[22] Zhen Zhang, Xiangdong Ding, Junkai Deng, Jian Cui, Jun Sun, Tetsuro Suzuki, Kazuhiro Otsuka, and Xiaobing Ren, The Journal of Physical Chemistry C **117** (15), 7895 (2013).

[23] Zhen Zhang, Xiangdong Ding, Jun Sun, Tetsuro Suzuki, Turab Lookman, Kazuhiro Otsuka, and Xiaobing Ren, Phys. Rev. Lett. **111** (14), 145701 (2013).

[24] Hongxiang Zong, Ze Ni, Xiangdong Ding, Turab Lookman, and Jun Sun, Acta Mater. **103**, 407 (2016).

[25] Ruben Mas-Balleste, Cristina Gomez-Navarro, Julio Gomez-Herrero, and Felix Zamora, Nanoscale **3** (1), 20 (2011).
[26] S. Nosé, J. Chem. Phys. **81** (1), 511 (1984).
[27] W. G. Hoover, Phys. Rev. A **31** (3), 1695 (1985).
[28] M. Parrinello and A. Rahman, J. Appl. Phys. **52** (12), 7182 (1981).
[29] S. Plimpton, J. Comput. Phys. **117** (1), 1 (1995).
[30] Wei Gao and Rui Huang, J. Mech. Phys. Solids **66**, 42 (2014).
[31] Suzhi Li, Qunyang Li, Robert W. Carpick, Peter Gumbsch, Xin Z. Liu, Xiangdong Ding, Jun Sun, and Ju Li, Nature **539** (7630), 541 (2016).

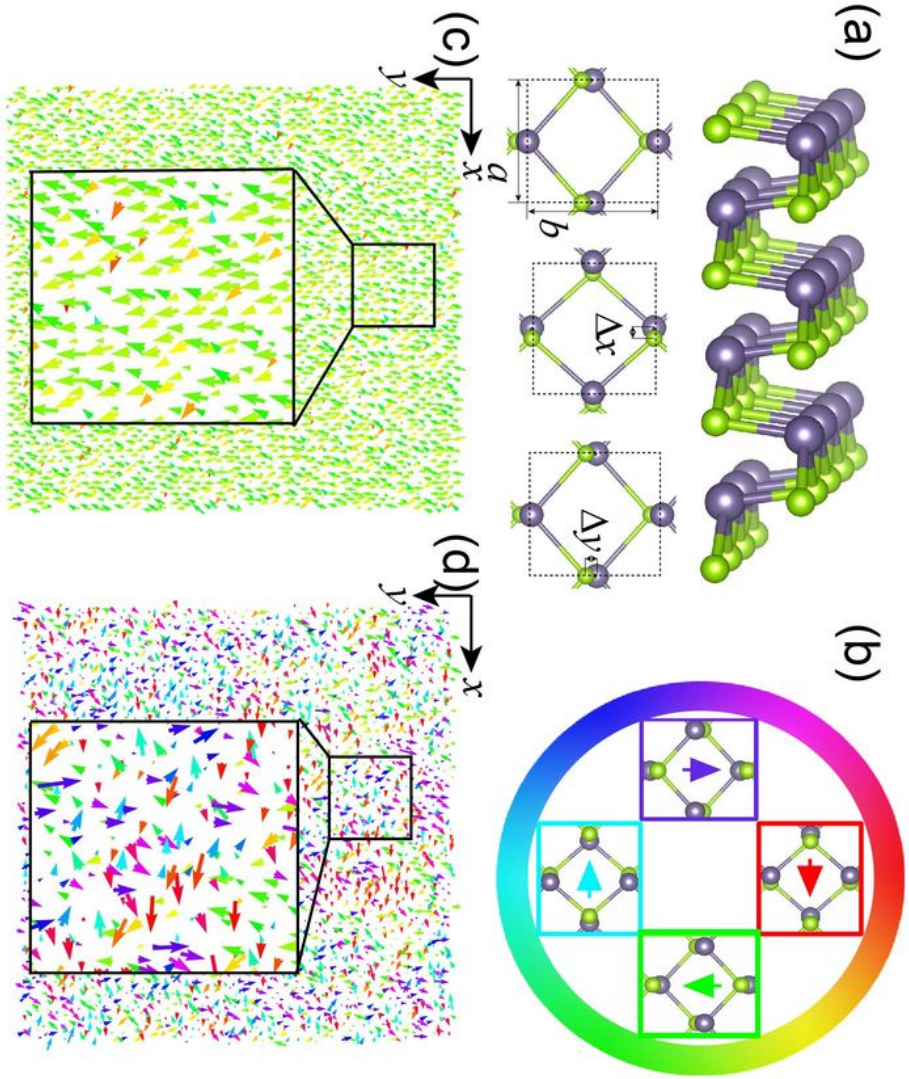

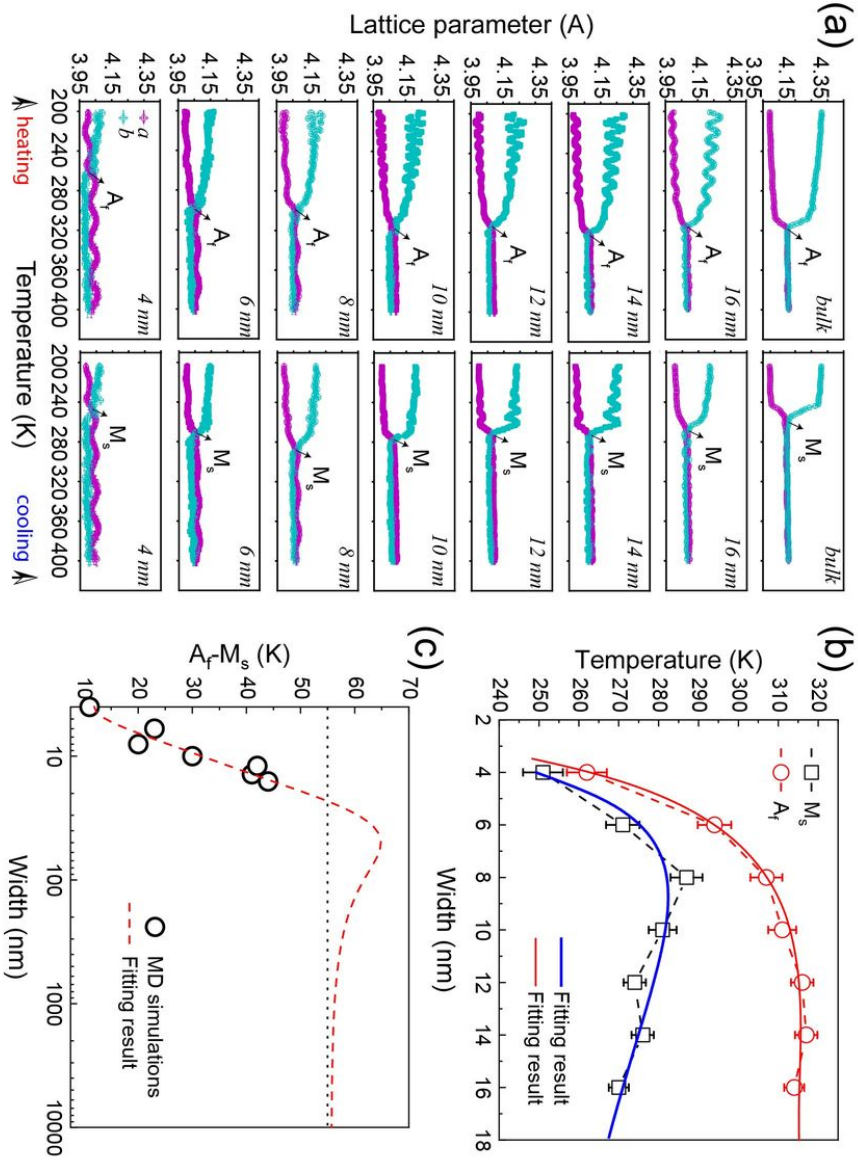

PLEASE CITE THIS ARTICLE AS DOI: 10.1063/5.0111375

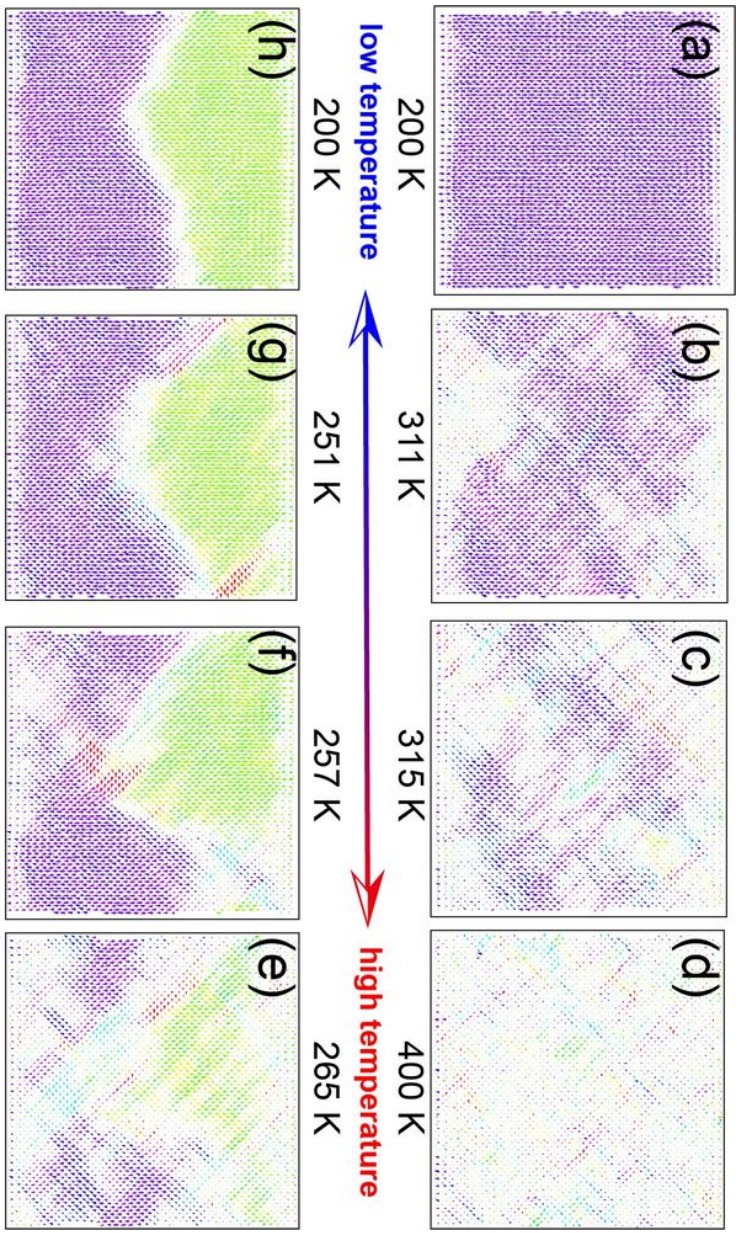

PLEASE CITE THIS ARTICLE AS DOI: 10.1063/5.0111375